Surface Characteristics of Martian Lobate Debris Aprons: Insights from HiRISE Images and Topography

Abstract no. 2962

E.C.S. Joseph, A.V. Pathare, D.A. Crown, D.C. Berman, F.C. Chuang, Planetary Science Institute, 1700 E. Ft. Lowell Rd., Suite 106, Tucson, AZ 85719; ejoseph@psi.edu.

1. Introduction

As lobate debris aprons (LDAs) are significant reservoirs of ancient ice on Mars, the formation and modification of their surfaces provide important clues to Martian climate history. Studies of LDA surface textures [1-5] indicate a complex history, including deposition of ice-rich mantles during the Amazonian Period, and subsequent degradation of the mantle by aeolian modification and ablation of contained ice. Past work evaluated surface textures at the Mars Global Surveyor's (MGS) Mars Orbiter Camera's (MOC) ~2-12 m/pixel and Mars Reconnaissance Orbiter (MRO) ConTeXt Camera's (CTX) ~5-6 m/pixel resolution [1, 2, 6]. This work extends LDA surface texture analyses to images from MRO's High Resolution Imaging Science Experiment (HiRISE), enabling a more detailed evaluation of surface degradation and modification.

Previous studies [1, 3] identified a topographical component to the surface textures, with degradation of the mantled surface gradually removing material and decreasing the thickness of the apron (Figure 1a). The current work incorporates the generation of Digital Terrain Models (DTMs) from stereo HiRISE pairs (using the method described in [7]) in order to more precisely study the relationship between LDA surface texture and topography.

This study begins the work of increasing the number of aprons with mapped surface textures, expanding that mapping to HiRISE resolutions, and combining these data with the topographical analysis of DTMs. Two examples, both from the area east of Hellas Planitia, are presented:

- Apron I (Figure 2): Debris apron complex extending from a massif into an impact crater located at 102.7 E, 38.9 S. Also Apron 9 in [9], East Hellas Apron B in [1], and hourglass-shaped deposit in [10] (See Figure 1b).

-Apron II (Figure 3): Massif-encircling apron located at 102.9 E, 40.6 S. Also Apron 2 in [9], East Hellas Apron A in [1], and massif discussed in [11].

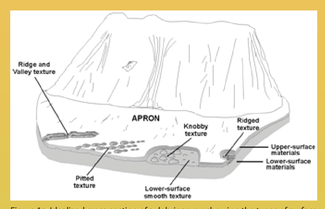

Figure 1a: Idealized cross-section of a debris apron showing the types of surface textures identified in analyses of MOC images [from 3]. The upper-surface materials are inferred to be a mantling deposit of ice and debris that overlies thicker lower-surface apron materials. Textures develop within the upper surface material as it degrades. Note: material thickness and textural features not drawn to scale.

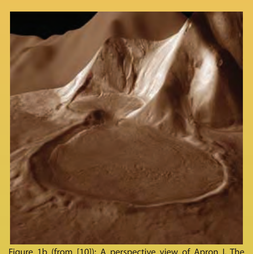

Figure 1b (from [10]): A perspective view of Apron I. The source massif is ~3.5 km high. Images from the High Resolution Stereo Camera, vertical exaggeration ~30x.

2. Degradational Textures

The mantled surfaces of debris aprons have been observed to display an established suite of textures interpreted to be caused by mantle degradation at MOC/CTX resolution [1-6]. These textures are characterized as being part of either Upper or Lower suites of textures. The Upper textures are interpreted to be part of the topmost, mantled surface layer (in various degrees of degradation), and the Lower textures are underlying materials exposed by degradational processes.

Upper Smooth Material (**USM**) is considered to be the least degraded of the textures, preserving the smooth surfaces of mid-latitude mantling deposits. Progressive degradation by aeolion activity and the sublimation of volatiles is interpreted to create the textures Upper Pitted (**UPT**), Upper Ridge and Valley (**URV**), and other upper textures as the mantle breaks down.

Further erosion and removal of mantle material form transitional textures such as Pitted, Ridge and Valley (**PTRV**) and Pitted, Ridge and Valley, and Knobby (**PTRVKB**).

The lower textures may represent the original surface of the lobate debris apron which is being revealed by the excavation of the mantle. Lower textures include Lower Smooth Material (**LSM**), Lower Knobby (**LKB**), and Lower Sharp Ridge (**LSR**).

These textures are observed to be gradational, i.e. lacking sharp contacts, as shown in Figure 2a, where the demarcation between **USM** and **UPT** is indistinct.

Apron I

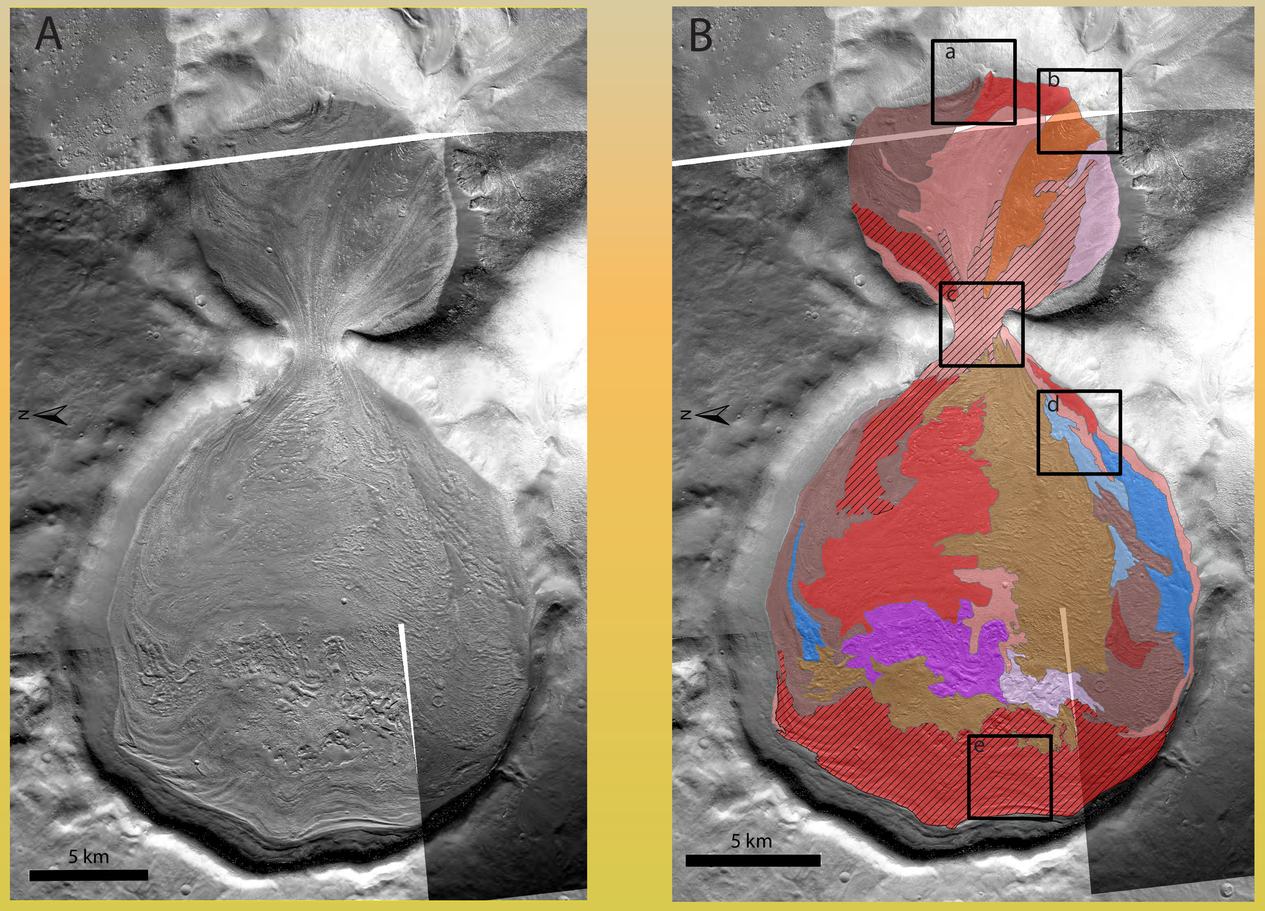

Figure 2: Apron I, shown (A) in CTX images F07_038490_1424_XI_37S257W and F06_038490_1424_XI_37S257W; NASA/JPL/MSSS, and (B) with surface texture maps. See Figures a-e for detailed images of the areas indicated by the black squares.

3. Flow Textures

In addition to the degradation of the mantle, the surfaces of lobate debris aprons are modified by the motion of the apron itself. This deformation manifests in the surface textures in two ways: either (1) as a modification of one of the degradational textures or (2) with textures whose formation is dominated by flow. Apron I provides examples of both.

Two degradational textures show evidence of flow in this apron, Upper Smooth Material (**USM**), visible in Figures 2c and 2e, and Upper Pitted (**UPT**), shown in Figures 2b and 2c. In these areas, the degradational textures are clearly visible (compare Figure 2d), along with lineations that are attributed to flow. These modified textures are indicated by hatching in Figure 2B, and by the addition of '**+F**' to the texture labels.

Figure 2e also shows a different indicator of flow - elongated craters. This section of apron abuts the far western wall of the containing crater, and this contact has caused compression of not only its **USM** texture, but several small craters. These craters are interpreted to have occurred before emplacement was complete, with the subsequent motion of the surface altering their morphology,

For an example of a texture that is characterized by flow mechanisms rather than the degradation of the mantle, see the **Ridged** texture in Figure 2b. This area appears to be a distinct lobe, with a flow direction that varies from the overall direction of emplacement. The texture is composed of concentric ridges which are parallel to the apparent direction of the lobe's flow. Examination of the topography of the source massif suggests a "tributary" source in this area, supplementing the main material flow.

These marks of flow are invaluable for understanding the formation processes of lobate debris aprons, offering a test mechanism for an associated effort to numerically model apron formation, as described in [8].

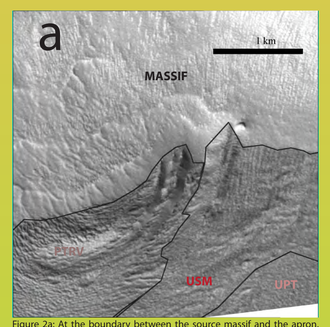

Figure 2a: At the boundary between the source massif and the apron, progressive degradation is clearly visible. On both the massif and apron, the degree of erosion increases to the north (left in the image), with Upper Smooth Material (USM) and a similarly smooth source texture giving way to a Pitted Ridge and Valley (PTRV) textured area of the apron and sharp ridges being exposed on the source slope.

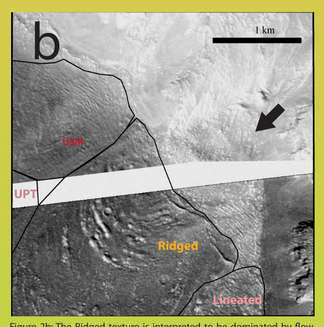

Figure 2b: The Ridged texture is interpreted to be dominated by flow rather than the erosion of the mantle. The concentric ridges of this lobe are parallel to the apparent direction of emplacement, which is different from the apparent direction of the overall emplacement of the apron. Examination of the source slope suggests a "tributary" source of material flowing through a local topographic low, supplementing the main source slope.

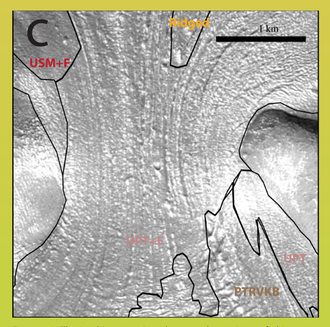

Figure 2c: The 'neck' connecting the two depressions of this apron complex is an area of severely constricted flow. This is evident in the modification of the Upper Smooth Material and Upper Pitted Material by pronounced flow lineations. The lineations disrupt the 'classic' degradational textures. as seen by the transition between UPT and UPT+F in the lower right of the image.

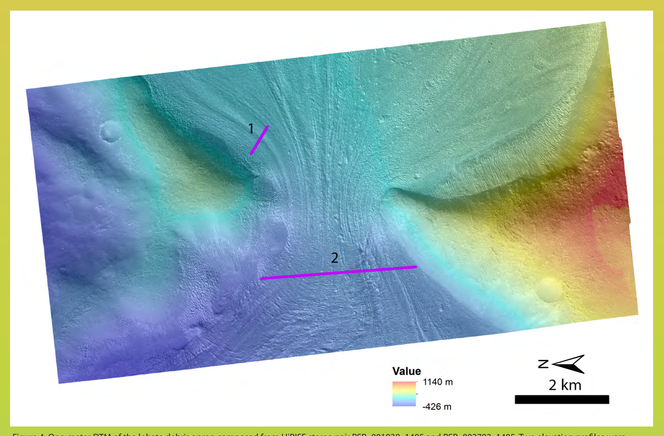

Figure 4: One-meter DTM of the lobate debris apron composed from HiRISE stereo pair PSP_001938_1405 and PSP_002782_1405. Two elevation profiles were drawn along the purple paths, which are shown in Figures 4a & 4b. Elevation Profile 1 (Figure 4a) traces path 1 from northwest to southeast, and Elevation Profile 2 (Figure 4b) traces path 2 from north to south.

Apron II

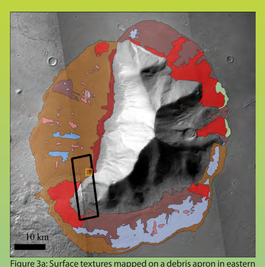

Figure 3a: Surface textures mapped on a debris apron in eastern Hellas, 102.9°E and 40.6°S [1]. (CTX images P16_007397_1382, G16_024552_1394, G15_023998_1393; NASA/JPL/MSSS). The black box indicates the footprint of the HiRISE stereo pair used to generate Figure 3d. The orange box shows the location of Figure 3b.

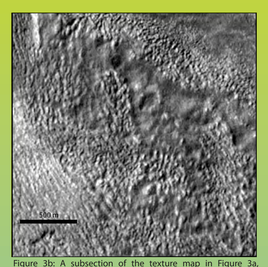

Figure 3b: A subsection of the texture map in Figure 3a, showing an area of Pitted/Ridge & Valley (PTRV) texture.

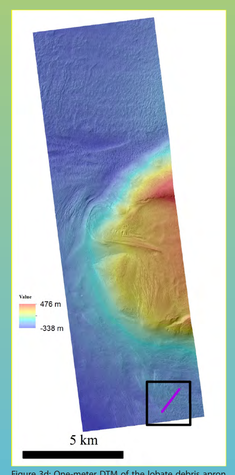

Figure 3d: One-meter DTM of the lobate debris apron composed from HiRISE stereo pair ESP_032978_1390 and ESP_033400_1390, showing the location of Figure 3c and the elevation profile shown in Figure 3e.

The inclusion of HiRISE data in the study of apron textures has allowed further insight into the aprons' history. Apron II's textures (Figure 3a) were mapped on CTX images in [1]. Figure 3b shows a section of the apron that has a Pitted/Ridge & Valley (**PTRV**) texture.

HiRISE images provide additional evidence of this gradational nature. The black box in Figure 3a denotes the footprint of a HiRISE stereo pair, which was used to create a HiRISE-based texture map in this section of the apron. The majority of textures observed using HiRISE may be characterized as "sub-textures" of the CTX-based textures, as in Figure 3c. This portion of the apron was considered to be composed of a single texture when mapped using CTX, but on HiRISE images it is divided into two textures, "Knobby", and "Smooth", where Smooth is interpreted to degrade into the Knobby texture.

The stereo pair was also used to construct a one-meter DTM (Figure 3d) using Socet Set software following the methodology described by [7]. An elevation profile was traced along the violet line in Figures 3c & 3d from the northeast to southwest, crossing the Knobby and Smooth textures. The results of the profile (Figure 3e) support the interpretation of the Smooth texture, with a higher elevation, degrading into Knobby as material is removed from the apron.

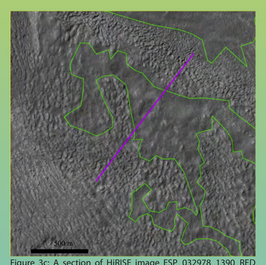

Figure 3c: A section of HiRISE image ESP_032978_1390_RED showing Smooth and Knobby textures on the apron's surface. The violet line shows the path of the elevation pro le in Figure 3e.

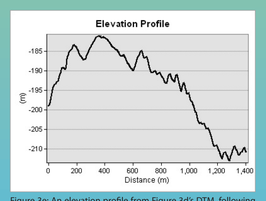

Figure 3e: An elevation profile from Figure 3d's DTM, following the path shown in Figure3c (NE-SW).

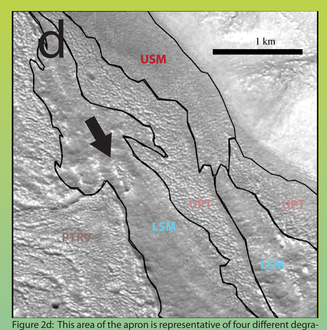

Figure 2d: This area of the apron is representative of four different degradational textures. The western edge of the apron (up in the image) is well-preserved and displays the Upper Smooth Material (USM) texture. As distance from the apron boundary increases, sublimation pits begin to appear, forming the Upper Pitted (UPT) texture. Two areas where the mantle has been largely removed show the Lower Smooth Material. Note the "island" of pitted mantle remaining in the depression. On the other side of the depression, there is an area of Pitted, Ridge & Valley (PTRV) texture.

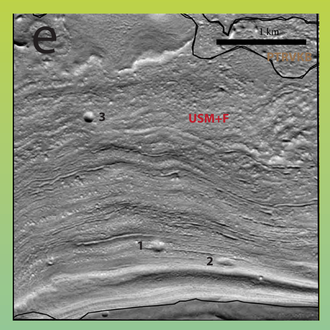

Figure 2e: This area of Upper Smooth Material is located at the far edge of the apron complex. This proximity to the western wall of the crater has resulted in compression of the apron, deforming the smooth mantled surface with lineations perpendicular to the direction of flow. Further evidence of this compression is in the shape of the westernmost impacts (1 & 2) on the apron, which are elongated from the circular morphology of the apparently younger impact towards the top of the image (3).

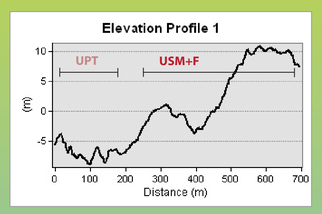

Figure 4a: An elevation profile following path 1 in the Figure 4 DTM from NW to SE. This profile demonstrates the difference in surface roughness between the Upper Pitted texture (UPT) and the better-preserved Upper Smooth Material (USM+F). The flow lineation is also clearly visible as a dip within the smooth region at ~400m.

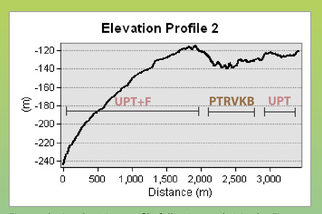

Figure 4b: An elevation profile following path 2 in the Figure 4 DTM from N to S. The greater degradation of the Pitted/Ridge & Valley/Knobby texture (PTRVKB) is apparent in this profile as a topographic low as compared to the Upper Pitted (UPT) terrain on either side.

References & Acknowlegdments

[1] Joseph, E.C.S., Crown, D.A., Chuang, F.C., Berman D.C. (2014) LPSC XLIV, abstract no. 2774. [2] Chuang F.C. and Crown D.A. (2005) Icarus, 179, 24-42. [3] Chuang F.C. and Crown D.A. (2012) LPS XLIII, abstract no. 2235. [4] Mangold, N. (2003) JGR 108, doi: 10.1029/2002JE001885. [5] Pierce T.L. and Crown D.A. (2003) Icarus, 163, 46-65. [6] Chuang F.C., et al. (2013) LPS XLIV, Abstract #2512. [7] Kirk, R.L., et al. (2008) JGR Planets 113, doi: 10.1029/2007JE003000. [8] Pathare, A.V., et al. (2016) LPS XLVII, abstract no. 2563, this volume. [9] Berman, D.C., Crown, D.A., Joseph, E.C.S. (2015) Planetary and Space Science, doi:10.1016/j.pss.2015.03.013. [10] Head, J.W., et al. (2005) Nature 434, doi:10.1038/nature03379 [11] Brough, S., et al. (2015) Journal of Maps, doi: 10.1080/17445647.2015.1047907

This work is supported by grant NNX15AM54G from NASA's Mars Data Analysis Program.